Journal of Sedimentary Research

Journal of Sedimentary Research, 2010, v. 80, 119–128
Research Article
DOI: 10.2110/jsr.2010.005

note Erratum at end of paper

LENTICULAR SHALE FABRICS RESULTING FROM INTERMITTENT EROSION OF WATER-RICH MUDS—INTERPRETING THE ROCK RECORD IN THE LIGHT OF RECENT FLUME EXPERIMENTS

JUERGEN SCHIEBER,[1] JOHN B. SOUTHARD,[2] AND ARNDT SCHIMMELMANN[1]
[1]*Department of Geological Sciences, Indiana University, Bloomington, Indiana 47405, U.S.A.*
[2]*Department of Earth, Atmospheric, and Planetary Sciences, Massachusetts Institute of Technology, Cambridge, Massachusetts 02139, U.S.A.*

ABSTRACT: **Lenticular lamination is a fabric that is known from shales of all ages, but its origin and paleoenvironmental significance is poorly understood. We have successfully reproduced this fabric in flume experiments. Beds of water-rich mud were eroded in a flume and yielded sub-millimeter to centimeter-size fragments that can be transported in bedload for distances of ten kilometers or more. Upon redeposition and compaction, these deposits have the same textural qualities as lenticular laminated shales from the rock record. Although accumulation of fecal pellets or abundant burrow tubes in a shale may produce comparable fabrics upon compaction, these can be distinguished from erosion-produced lenticular lamination via petrographic criteria. Lenticular lamination in shales that is due to deposition of water-rich mud fragments most likely records intermittent erosion and transport of surficial muds by currents.**

INTRODUCTION

Shales and mudstones account for two thirds of the sedimentary rock record, are arguably the most poorly understood sedimentary rock type (Schieber 1998a), and yet contain a wealth of sedimentary features that can provide information about depositional conditions and sedimentary history (O'Brien and Slatt 1990; Schieber 1986; Schieber 1989, 1998b). At present, however, we lack the information that would allow us to link features observed in the rock record to measurable sets of physical variables in modern environments.

Because the various small-scale sedimentary structures seen in modern muds have not been observed in the making, we are forced to infer controlling parameters (e.g., current velocity, density of suspension, etc.) from temporally and spatially very limited measurements in the overlying water column (e.g., Kuehl et al. 1986, 1988; Kuehl et al. 1991; Segall and Kuehl 1994). The tacit assumption, however, that measurements of today's conditions can be taken as representative of the uppermost centimeters to decimeters of modern sediments is contradicted by the inherent heterogeneity of most "modern" sediments (Kuehl et al. 1991). Currently our knowledge of modern mud deposition is two-dimensional and rather spotty, but interpretation of the rock record requires a three-dimensional solution. Detailed studies of modern environments may alleviate some of these problems, and further improvement is likely to come from experimental studies of mud deposition. This is not unlike the situation in sandstone sedimentology, where critical insights are owed to quantitative constraints that resulted from numerous flume studies (e.g., Allen 1982; Middleton and Southard 1984).

In this contribution we focus on a common shale fabric, so called "lenticular lamination" (O'Brien and Slatt 1990). Lenticular-laminated shale possesses a "flaser bedding" appearance and consists of lenses of variable composition that are arranged in wavy layers. Lenticular laminated shales occur from the Precambrian (e.g., Schieber et al. 2007a) onward (e.g., Wignall 1994). Many Phanerozoic black shale units show this fabric (e.g., O'Brien and Slatt 1990), and it also occurs in shales with low organic-matter content. Yet, even though it is a common fabric, its origin is poorly understood. Proposed origins include redeposition of shale rip-up clasts (Schieber et al. 2007a), packed fecal pellets (Röhl et al. 2001; Schmid-Röhl et al. 2002), and compaction of closely spaced burrows (e.g., O'Brien and Slatt 1990).

Work on lenticular fabric in Middle Proterozoic shales (Schieber et al. 2007a) allowed us to exclude fecal pellets and bioturbation as underlying causes, and to focus on redeposition of shale rip-up clasts as a formative process. Nonetheless, we were still faced with questions about the original water content and the state of induration of these clasts. Water-rich surficial muds contain as much as 90 volume percent water (e.g., Soutar and Crill 1977; Schimmelmann et al. 1990; Parthenaides 1991) and have "almost no shear strength" (Sheu and Presley 1986). There was therefore the long-standing assumption that such sediments "testify to the virtual absence of bottom currents" (Wignall 1994), and that they will be resuspended upon erosion. Experimental work by Einsele et al. (1974) showed erosion of clay clasts from kaolinite beds with approximately 60 to 65 volume percent water, also suggesting that some consolidation is needed before muds can erode in chunks instead of simply being resuspended.

In the rock record, mudstone clasts that are thought derived from a partially consolidated or lithified substrate tend to show rounded edges (Fig. 1), and if elongate are typically flattened parallel to bedding (Wignall 1989). Lenticular lamination, such as seen in Proterozoic shales (Schieber et al. 2007a) and various Phanerozoic examples (O'Brien and Slatt 1990), differs texturally (Fig. 2) from beds of redeposited semilithified mudstone clasts (Fig. 1). The purported clasts do not show rounded edges, but instead are characterized by lateral pinch-out (Fig. 2). The latter feature implies much more postdepositional compaction than what one would expect from partially consolidated mudstone clasts, and suggests that the clasts in question were eroded from a substrate with a comparatively high water content.

Because the latter conclusion is at variance with the notion that water-rich surficial muds should not form transportable clasts upon erosion

 1527-1404/10/080-119/$03.00

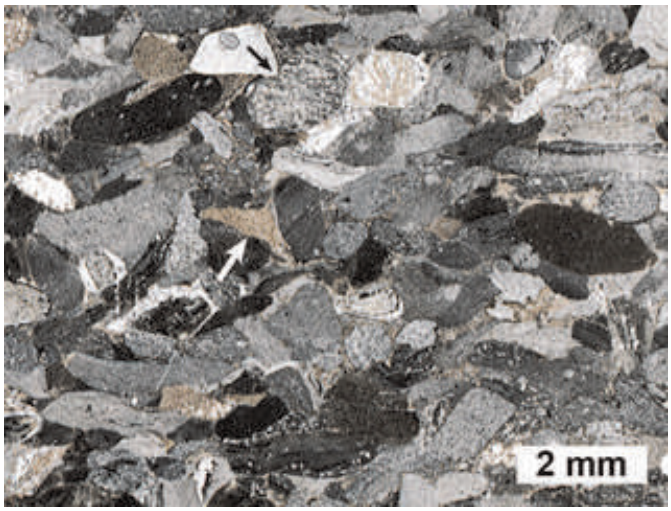

FIG. 1.—Example of a shale clast deposit from the Proterozoic Belt Supergroup in Montana. The clasts are rounded at the edges, implying transport and rounding. Clasts have been deformed around harder grains (black arrow) and have been squeezed into pore spaces (white arrow), suggesting that they were not fully lithified. Vertical compaction of clasts is minor, however, indicating that these clasts were remobilized from deposits that had undergone considerable compaction. The compaction state and deformation of clasts in this example contrasts strongly with deposits formed from soft water-rich clasts that are the focus of this study.

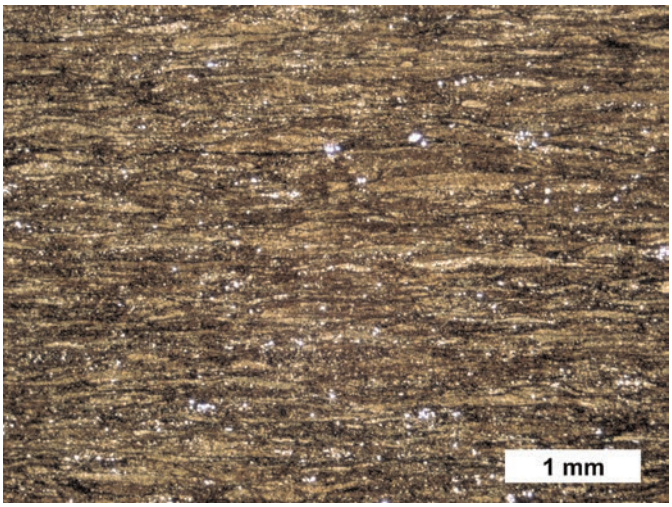

FIG. 2.—An example of lenticular lamination in a shale. Photomicrograph from a thin section of the Proterozoic Rampur Shale (Proterozoic of India, described by Schieber et al. 2007a).

because they lack shear strength, we conducted flume experiments to explore this issue further. In this contribution we present observations that demonstrate that watery muds do indeed yield clasts that can be transported and redeposited and discuss the implications for interpreting the rock record.

METHODS

The racetrack flume we used for our experiments (Schieber et al. 2007b) has a 25-cm-wide channel, a 7.2 m straight observation stretch, and turning sections with 1.5 m radius. The observation stretch and the upstream turning bend were covered with a flow lid at 10 cm above the flume bottom (5 cm effective flow depth). The turning bends also contained two parallel vanes to reduce the development of secondary circulations. A diffuser was placed at the upstream end of the observation section. The water is moved by a paddle belt that engages the flow over a distance of about 6 meters. The design differs from past experimental studies in which centrifugal pumps were used to recirculate mud suspensions (Hawley 1981; Pasierbiewicz and Kotlarczyk 1997; Baas and Best 2002). In the latter case, destruction of floccules and clay bed fragments by high shear forces in the pump represent a significant departure from natural conditions. Our flume was specifically designed to not unduly interfere with fragile particles during transport and deposition (Schieber et al. 2007b), and thus to allow for a closer approximation to transport and flow conditions in natural environments.

We conducted two erosion experiments with kaolinite (91% finer than 0.01 mm, 80% finer 0.005 mm, and 60% finer than 0.002 mm). In each experiment the clay was mixed with water and stirred in a blender for 10 minutes. The blended slurry was then washed trough a 63 μm sieve directly into the flume, flocculated, and formed ripples that accreted into clay beds (Schieber et al. 2007b). In the first experiment 500 g of kaolinite were added to the flume, and in the second experiment 6000 grams were added. In the latter case 1000 gram increments were added over six days, with each clay increment stained with a different color. This was done so that the colored layers could provide a range of contrasting clay clasts for redeposition.

Average flow velocity was measured with a Marsh-McBirney Flowmate 2000 flow meter (1 inch diameter sensor head) in mid-channel at 5 cm above the channel bottom. Near-bed flow velocities and velocity profiles used for shear-stress estimates (Middleton and Southard 1984) reported here were measured with a Sontek MicroADV (acoustic Doppler velocimeter) instrument in a later experiment that was geometrically identical. Recent studies of muddy flows have shown that high mud concentrations (in excess of 10 grams per liter) affect viscosity (Baas and Best 2002) and thus lead to departures from the traditional logarithmic velocity profile and to potential errors when shear stress is estimated via velocity profiles. In our experiments, however, we operated at suspended-sediment concentrations of less than 0.1 grams per liter, far less than necessary to affect viscosity.

Unlike linear flumes, a racetrack flume can not be tilted to achieve uniform flow depth. We therefore use a flow lid to ensure uniform flow across the length of the channel. With the flow lid 10 cm above the flume bottom, our effective flow depth is 5 cm. Vertical and lateral velocity profiling shows that except for a 10 mm zone along the wall, the velocity profile is essentially flat across the channel. Thus, the mid-channel velocity measured at 5 cm depth represents a good approximation of the average flow velocity. The flow is fully turbulent, as indicated by Reynolds numbers that range from 6,770 at 15 cm/s to 11,280 at 25 cm/s for an effective flow depth of 5 cm and 25° C.

After accretion of the mud bed we stopped the flume and allowed the deposit to consolidate for 2 weeks and 9 weeks, respectively. Samples were taken from both clay beds and the water content was determined gravimetrically. Multiple samples from both beds showed their water content to be approximately 70% by weight (~ 85% by volume) in both cases. Following consolidation we stepped up flow velocity until erosion of the mud bed occurred, and simultaneously monitored the process with time-lapse and video cameras.

Deposits of clay bed debris were collected with shallow containers that had been placed downstream of a flow baffle in the flume channel and were stabilized with Spurr low-viscosity epoxy resin (Spurr 1969; Smith and Anderson 1995). Pore waters were sequentially exchanged for acetone, and then the acetone was sequentially exchanged for Spurr resin (Polysciences Inc.). The resin-infused sample was then cured at 60°C for 24 hours, cut into slices, polished, and photographed. For comparison

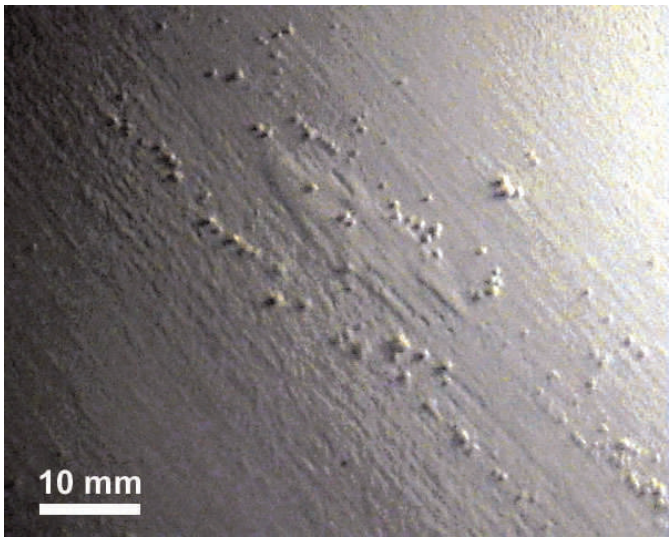

FIG. 3.— Video frame from experimental erosion of thin flume-deposited clay bed (flow velocity = 16 cm/s, flow depth = 5 cm). Initial products of erosion are small clay rip-ups that travel across the flume bottom (view from above) and become well rounded within 1–2 trips around the race track (a distance of 25–50 m). The size of visible fragments ranges from 0.5 to 2 mm.

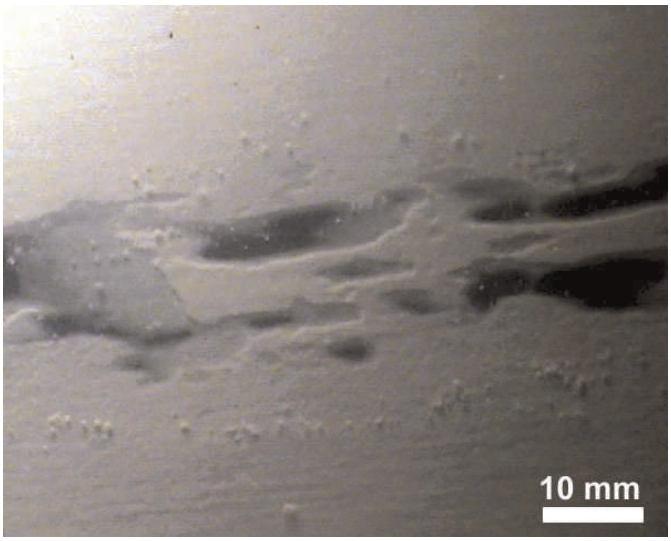

FIG. 4.— Video frame from experimental erosion of thin flume-deposited clay bed (flow velocity = 17 cm/s, flow depth = 5 cm). Erosion of clay bed is clearly visible in the center portion of the image (view from above). The image also shows that the clay deposit has internal layering and that at a given location erosion strips off one layer at a time. The size of visible fragments ranges from 0.5 to 2 mm.

with the rock record we chose samples from the first author's collection of petrographic thin sections. To compare our uncompacted experimental samples to the rock record, we used Photoshop to "virtually" compact images of cut surfaces (Lobza and Schieber 1999).

We also wanted to compare these deposits with those resulting from redeposition of clasts derived from more indurated muds. We prepared a thin sheet of plastically behaving kaolinite with 30 vol% water, and then chipped small centimeter-size pieces into the flow at 25 cm/s. The chips traveled down the channel, variably broke up into smaller pieces, and accumulated in our collection containers. The collected material was then processed with Spurr resin as described above. The clay clasts absorbed water while submerged, and their water content at the time of sampling was approximately 40% by volume (determined gravimetrically).

OBSERVATION OF BED EROSION

When eroding the first clay bed (500 g kaolinite, 2 week consolidation), signs of erosion appeared at a flow velocity of 16 cm/s. Small clay rip-ups began to travel along the flume bottom (Fig. 3). Initially of irregular shape, they became rounded after traveling around the track once or twice and formed clay balls of 0.5 to 2 mm size. At a flow velocity of 17 cm/s, portions of the clay blanket on the flume bottom gradually eroded (Fig. 4) and turbidity slowly increased. Erosion occurred in steps, peeling off irregular (millimeter to sub-millimeter size) pieces first from the topmost layer, and as erosion progressed from layers deeper in the deposit (Fig. 4). The irregular fragments of the eroding clay blanket were recast as traveling clay balls instead of simply being resuspended. Most of the eroded material traveled as bedload, turbidity increased only slightly, and this allowed us to film and photograph clay transport and erosion features (Figs. 3, 4). Thus, although the clay bed was deposited from a turbid and opaque suspension, current erosion did not resuspend and disperse the bulk of the previously deposited material. As flow velocity was increased further, the extent of erosion increased only modestly until a flow velocity of 20 cm/s was reached. When flow velocity was stepped up gradually from 20 cm/s to 26 cm/s, clay bed erosion expanded steadily and the turbidity increase rendered the flow opaque. Finally, at 26 cm/s the last remains of the clay bed were removed from the flume bottom. Turbidity increases reflect initially abrasion of the bed because "breaking out" of fragments is accompanied by production of smaller particles that enter the overlying flow, but over longer time periods the breakup of larger clasts contributes an increasing proportion of the suspended sediment.

In the case of the second clay bed (6000 g kaolinite, 9 weeks consolidation), the pre-erosion average turbidity at 10 cm/s was 34.6 mg/l, a turbidity level that allows a clear view across the flume bottom. As in the prior erosion test, the first signs of erosion occurred at 16 cm/s. Irregular shreds were torn from the topmost layer of the bed and formed rounded rip-ups in the 0.5 to 2 mm size range as they traveled down the channel. Turbidity rose slightly to 36.4 mg/l and stabilized. As velocity was gradually ramped up to 20 cm/s additional erosion increased the population of traveling clay balls, and turbidity increased gradually but stabilized after each velocity step (at 20 cm/s turbidity stabilized at 38.4 mg/l). Increasing velocity to 23 cm/s again led to an increase in traveling fragments, as well as a slight increase in turbidity followed by stabilization (at 23 cm/s turbidity stabilized at 43.7 mg/l). Finally, once the velocity reached 26 cm/s, we observed a rapid climb of suspended-sediment concentration and the flow became fully opaque (at a turbidity of $\sim$ 50 mg/l). The turbidity increase slowed after reaching 70 mg/l, but there was a continued gradual increase of turbidity and sustained erosion and continued removal of sediment. At flow velocities above 26 cm/s the only observed change was an increase in the rate of erosion as indicated by the rise of turbidity over time. In this contribution, however, the focus is not on the factors that control erosion rates, but rather on the redeposition of clay rip-ups and the resulting deposits. For context, the flow velocities for erosion and rip-up production in our experiments, 16 to 26 cm/s, are sufficient to transport medium sand and form sand ripples in our flume (Schieber et al. 2007b).

Average near-bed velocities were measured with a SonTek Micro ADV at 2 mm, 5 mm, and 10 mm above the bed (Fig. 5). From time lapse observations of fragments traveling over the eroding bed, average travel velocities (Fig. 5) for mm-size clasts ranged from $\sim$ 3 cm/s (15 cm/s average flow velocity) to 6 cm/s (25 cm/s average flow velocity). Observations made over extended time periods (12–24 hours) show that initially produced rip-up clasts gradually diminish in abundance. Clast

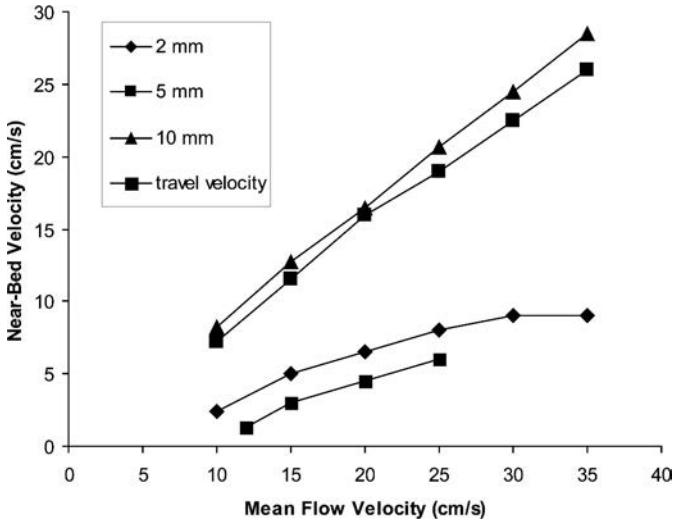

FIG. 5.—Average near-bed velocities at 2 mm, 5 mm, and 10 mm above the bed, relative to mean flow velocity. Measured in down-channel direction with a Sontek MicroADV instrument. The bottom curve indicates directly measured average travel velocities of clay rip-ups that moved over the bed surface (bedload particles).

abundances produced when stepping up velocity typically diminish to about half over the following 12–24 hours.

For the flow velocities used in our experiments, the bottom shear stress was estimated from well defined velocity profiles in the innermost part of the wall-law region. For the onset of bed erosion, at an average velocity of 16 cm/s, we derived a bottom shear stress of ~ 0.07 Pa. At an average velocity of 26 cm/s, the onset of continued bed erosion and clast disaggregation, the estimated bottom shear stress had increased to ~ 0.21 Pa (note that shear values were adjusted from original paper).

As pointed out above, when flow velocity reached 26 cm/s we observed a rapid and sustained increase of turbidity, a consequence of substantially accelerated erosion. Unfortunately, turbidity precluded us from making direct observations of the traveling particles and erosional features at that point. What we know of the produced particles derives from examination of the material preserved in our collection containers and in "point bar" deposits within the curved sections of the flume channel. Bed erosion features were observed after the turbid water of the flume had been drained and replaced with clear water.

Geometrically, the eroded clay bed resembles a yardang plain (Fig. 6A), reflecting erosion of a cohesive substrate by unidirectional flow (Breed et al. 1989). At closer inspection we see meandering, flow-parallel troughs that are eroded into clay strata, as well as the earlier observed layer-by-layer erosion of clay strata (Fig. 6B). Differential erosion of clay strata brings out minute detail, such as the cross-laminae of eroded floccule ripples (Fig. 6C, D), and the layering of successively deposited clay strata (Fig. 6D, E). At the time the images for Figure 6 were taken, the clay bed contained approximately 85 volume % water. In

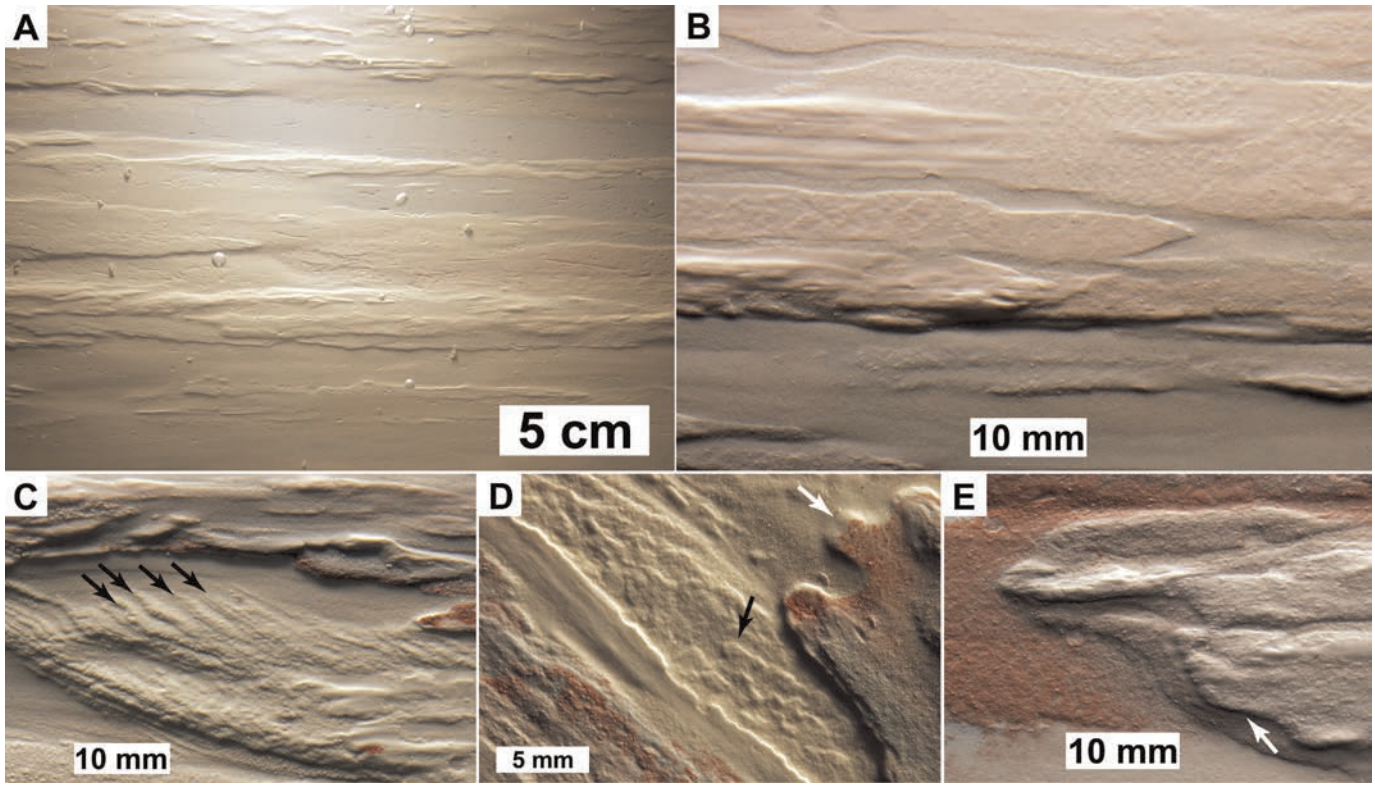

FIG. 6.—Erosion features observed on the second clay bed (6000 g kaolinite, 9 weeks consolidation) after erosion at 26 cm/s (view from above). **A)** longitudinal ridges and furrows parallel to flow direction. **B)** Close-up of Part A, showing narrow erosional furrows that cut into a resistant layer. The scale-like features to cover this layer are most likely the remains of floccule ripples (Schieber et al. 2007b) that have been eroded almost completely. **C)** Downcurrent-dipping foresets of a floccule ripple (arrows) have been exhumed by erosion. The irregular edges of eroded foreset laminae suggest discontinuous erosion in the form of fragments. Upper third of image shows differential erosion and undercutting of clay layers. **D)** Close-up near area of Part C. White arrow points to "cliff" that has been smoothly eroded, and black arrow points to example of irregularly eroded foreset lamina suggestive of discontinuous erosion as fragments. **E)** Differential erosion of clay laminae. There is clear undercutting of the uppermost lamina (arrow). Flow from left to right for all images except Part D, where flow is from the upper left to the lower right.

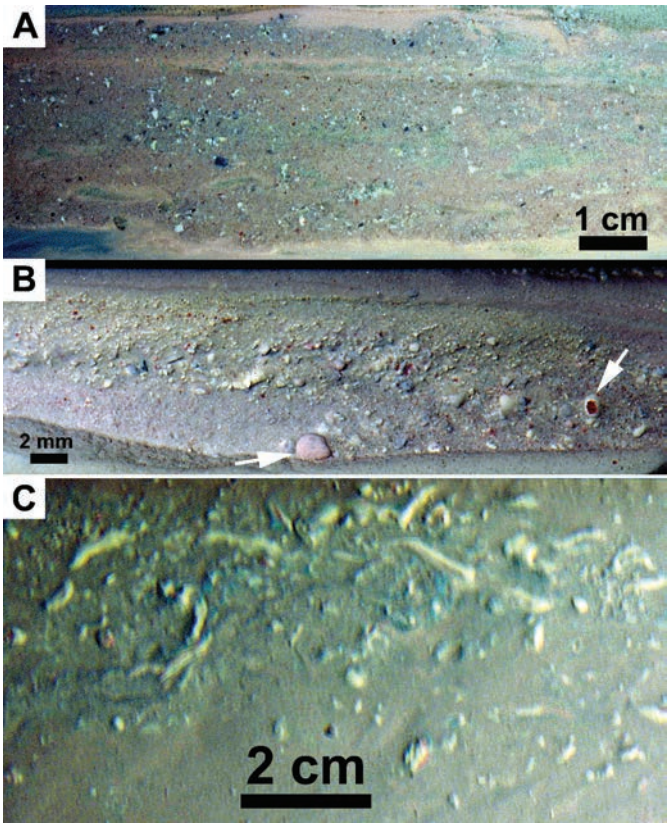

FIG. 7.—Redeposited clay rip-ups from erosion of second clay bed (view from above). **A)** Layer of variably colored clay clasts that range in size from a fraction of a millimeter to several millimeters (eroded at 26 cm/s over two hours). **B)** Clast-rich "point bar" deposit where several large clasts with well developed rounding are clearly visible (arrows). **C)** Accumulation of large irregular-shaped fragments (millimeter to centimeter size) that appear to consist of sheets of material which are variably deformed (eroded by short velocity burst of 30–35 cm/s).

areas where erosion had cut through the bed to the flume bottom, we were also able to observe the progress of erosion at the edge of the still-existing bed. Erosion was not continuous, but rather proceeded by intermittent removal of millimeter-size chunks of sediment.

We also wanted to get a better understanding of what the larger fragment sizes would be during erosion at velocities above 26 cm/s. By the time we had collected our clast samples for embedding in Spurr resin, there was a substantial clay bed left (Fig. 6A). We eroded this remaining clay bed with short bursts (1–3 minutes) of higher flow velocity (30–35 cm/s) and then shut off the flume before the fragments had a chance to be reduced in size by transport. This approach yielded abundant centimeter-size fragments as seen in Figure 7C. Fragments of this size were rarely observed during prior erosion runs that lasted an hour or more, suggesting that large rip-up clasts of soft clay are prone to disintegration and size reduction over comparatively short transport distances. We also observed the formation of localized deep and elongate erosional scours during these velocity bursts (Fig. 8). A few of these we could observe while they formed because they cut through the entire bed (Fig. 8). They start at localized scour pits, and over the space of a few minutes multiple centimeter-size chunks of sediment are ripped out of the bed in a downcurrent line.

OBSERVATION OF DEPOSITS

Erosion of the first clay bed provided visual evidence of clay-bed remobilization in the form of clay clasts that traveled in bedload, but did not provide enough material for sampling of deposits. In the more sediment-rich second experiment, clay rip-ups accumulated not only in the designated collection containers but also in other areas where flow velocity and/or turbulence was below average. One such area was in the region downstream of the drive belt (Fig. 7A, C). Also, because the downstream turning section did not have a flow lid, the effective flow depth changed from 5 cm to approximately 12 cm, causing a reduction in bottom shear stress and accumulation of sediment. Due to secondary flow in the turns, these deposits formed point-bar-like buildups on the inside of the bend (Fig. 7B).

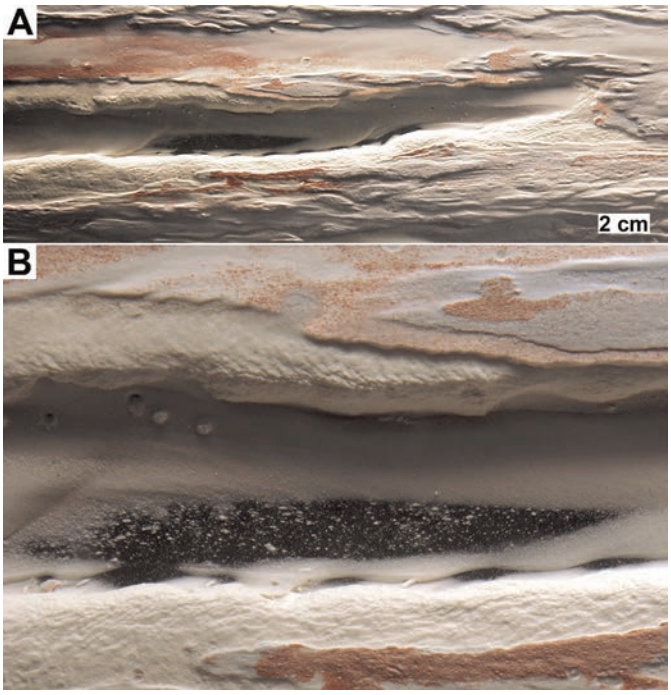

FIG. 8.—Narrow, deep scour in the second clay bed, produced by short velocity burst. Scour is about 2 cm wide and 1 cm deep (view from above). **A)** Overview of scour channel. Channel is partially filled with post-scouring sediment. **B)** Detail of channel walls that shows cross-lamination in the basal white kaolinite unit and differential erosion of overlying beds.

These clast deposits consist of a mixture of clay rip-up clasts from multiple stratigraphic levels (Fig. 7) and are poorly sorted. Clasts that were produced during extended erosion runs at 26 cm/s typically range in grain size from a fraction of a millimeter to approximately 2 millimeters (Fig. 7A, B). Figure 7B shows that these clasts are rounded during transport and largely in the sub-millimeter size range.

What these clast deposits look like once stabilized in Spurr resin and sectioned is shown in Figure 9. Surfaces cut perpendicular to bedding show irregular-shaped clumps piled on top of each other with their long axes generally subhorizontal (Fig. 9A). The space between clearly visible fragments is filled by clay floccules. Because floccules and clasts are of the same composition, contrast between clasts and matrix is not always strong. Contrast is best when clearly differently colored clasts are directly juxtaposed (e.g., Fig. 9C). Using Photoshop to "virtually" compact this image (Lobza and Schieber 1999) shows that the clay lumps flatten, are overall lenticular, taper out laterally, and result in an overall lenticular fabric (Fig. 9B, C).

Deposits recovered from burst erosion experiments are coarser grained, with many rip-up clasts in the 5 to 10 mm size range (Fig. 10A). "Virtual" compaction again results in flattened-lenticular clay lumps that taper laterally and produce a lenticular fabric (Fig. 10B). Some larger clasts were folded over during transport.

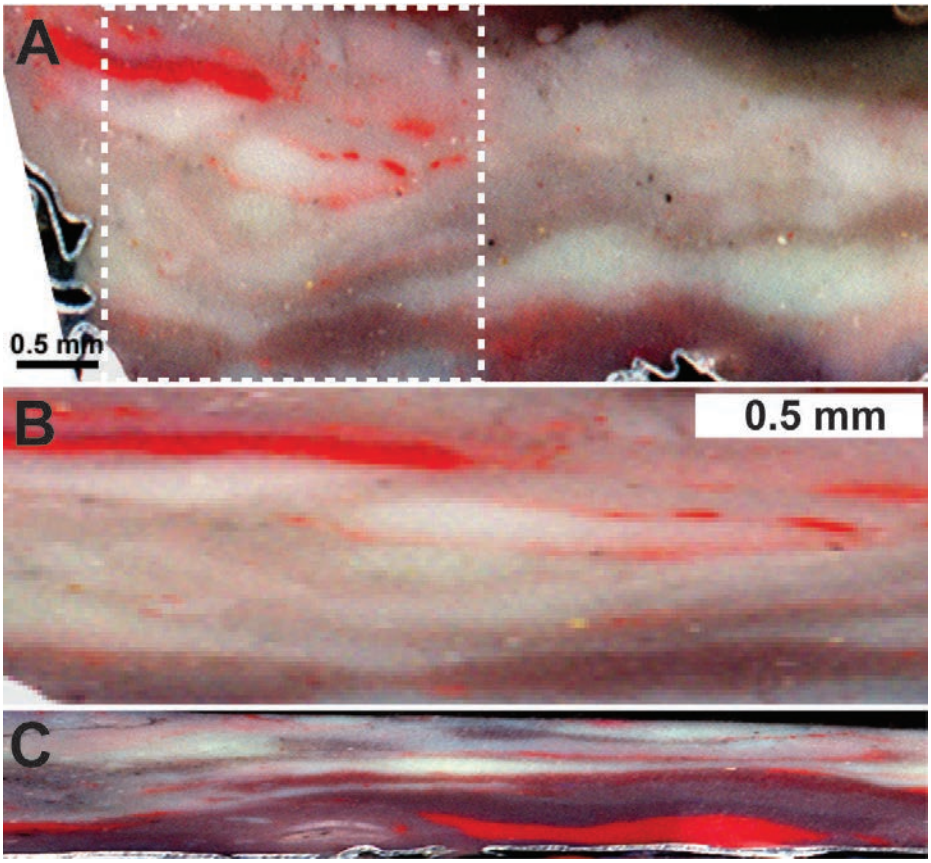

FIG. 9.—Spurr resin-impregnated clay-clast deposits from extended erosion at 26 cm/s. Original clasts are a few millimeters to a fraction of a millimeter in size. **A)** Uncompacted deposit that contained approximately 70 wt. % water (~ 85 vol %) before impregnation with resin. Note irregular-shaped clumps of clay material that are piled up on each other. The observed surface is perpendicular to bedding. **B)** The area delineated by dashed white line in Part A after "virtually compacting" it in Photoshop to 30% of original thickness (simulating compaction to 15% porosity). The clay clumps adopt a lenticular-tapering appearance and produce an overall lenticular fabric. **C)** Another example of lenticular fabric (same scale as in Part B), "compaction" to 30% of original thickness). The folded structures near the margins of image A are from sample containers fashioned out of aluminum foil.

Clast deposits produced from more indurated muds, chipped into the flow from a thin sheet of plastic kaolinite, are shown in Figure 11. Fragments range in size from sub-millimeter to more than a centimeter and are piled up irregularly in the original deposit (Fig. 11A). The clasts contained approximately 40 vol% water. When "virtually" compacted to 60% of their original thickness they still showed rounded edges, contrasting with the tapering and pinched appearance of the compacted water-rich clasts shown in Figures 9 and 10.

DISCUSSION

Gradually stepping up the flow velocity for our clay beds showed that one cannot really define a critical velocity when erosion sets in. Visible erosion started at 16 cm/s for both beds and led to a growing population of traveling clay rip-ups as velocity was ramped up. In the case of the first bed, each velocity step was followed by some more erosion and then a stabilization of the suspended-sediment concentration (turbidity), up to a flow velocity of 20 cm/s. The second clay bed behaved similarly up to a flow velocity of 24 cm/s. Thus, even though the second bed benefited from a substantially longer consolidation time, it showed itself to be only slightly more erosion resistant. The fact that gravimetric determination of water content (~ 70% by weight) for both beds shows no significant difference between them suggests that weeks vs. months of consolidation time makes little difference with regard to erodibility. Data summarized by Parthenaides (1991) support this conclusion and suggest that shear strengths of water-rich surficial muds are quite similar (approximately 0.02–0.03 Pa) regardless of consolidation state. These latter values mirror bottom shear stress values derived from velocity profiles in our flume (0.015–0.03 Pa). Thus, although we have to keep in mind that the mode of bed accretion (settling vs. current), clay type, grain-size distribution,

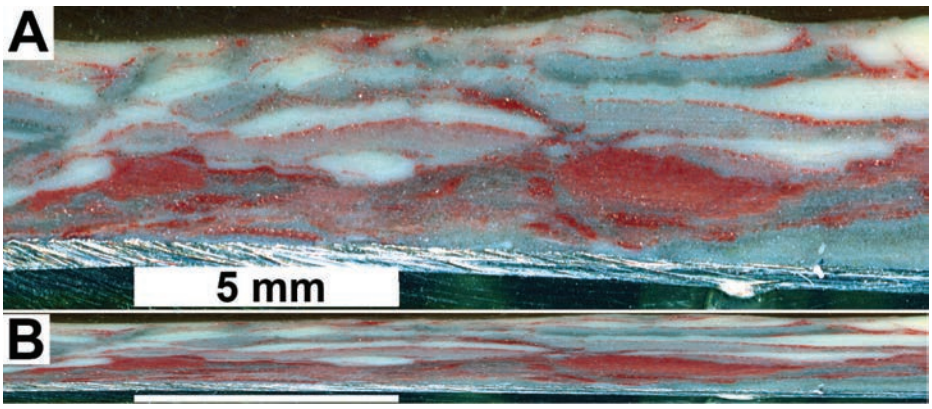

FIG. 10.—Spurr resin-impregnated clay-clast deposits produced by short erosion bursts (30–35 cm/s). Original clasts range in size from a few millimeters to 2 centimeters in size and are a few millimeters thick. **A)** Uncompacted deposit that contained approximately 70 wt. % water (~ 85 vol %) before impregnation with resin. The rip-up clasts are largely flat-oblate and pile up subhorizontally. The observed surface is perpendicular to bedding. **B)** The same image after "virtually compacting" it in Photoshop to 30% of original thickness. The clay clasts are now lenticular-tapering in appearance and lead to an overall lenticular fabric.

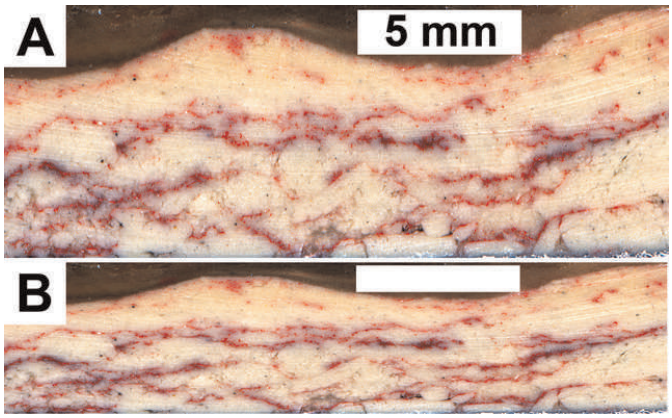

FIG. 11.— Spurr resin-impregnated clay-clast deposit produced from preconsolidated kaolinite. Original clasts range in size from a few millimeters to 2 centimeters in size and are a few millimeters thick. **A)** Uncompacted deposit that contained approximately 40 vol% water before impregnation with resin. The observed surface is perpendicular to bedding. **B)** The same image after "virtually compacting" it in Photoshop to 60% of original thickness. The clay clasts are flattened but still show rounded edges. This is in visible contrast to the lenticular-tapering appearance of water-rich clasts (Figs. 11, 12).

and a host of other factors can affect the erosional properties of mud beds (Berlamont et al. 1993), what we observed in our experiments may well be applicable to a wide range of modern surficial muds.

Our observations show that discontinuous erosion of clay beds in the form of rip-up clasts seems to be the norm, and that true resuspension of mud deposits occurs when these rip-ups are abraded during transport (rounding of clasts, Fig. 7B). As already observed by Einsele et al. (1974), formation of rip-up clasts appears to be aided by alternating layers of different erosion resistance and by bedding-plane discontinuities (Figs. 6, 8). Once erosion has started to "dig in" and weaken the bed, there is a tendency for the deposit to be "mined" in the downcurrent direction from that point. At lower flow velocities this may lead to elongate and meandering grooves that are a few millimeters wide and 1–2 mm deep (Fig. 6A, B), and at higher flow velocities it may produce downcurrent linear grooves that may be several centimeters wide and deep (Fig. 8). Compaction will render these features less obvious, but the former should result in subtle linear grooves, and the latter should result in millimeter-deep scour depressions. Both features have been observed by the first author on shale bedding planes in outcrop and in drill core.

Considering that clast abundances that resulted from stepping up velocity typically diminished to about half over the following 12–24 hours, we can assume that most of them likely would have vanished over a 48 hour period. Utilizing the travel velocities of bedload clasts measured in our experiments (Fig. 5), and assuming a flow velocity of 25 cm/s (travel velocity ~ 6 cm/s), a continuously traveling clast may traverse a distance of slightly more than 10 kilometers in that time span. Of course, sedimentary particles rarely travel continuously, and this figure should therefore be considered an estimate of maximum travel distance. The rapid increase in turbidity above flow velocities of ~ 25 cm/s suggests that at that point the disaggregation of clay rip-up clasts strongly accelerates and diminishes their prospect for transport over longer distances. Thus, the prospects for generating soft water-rich clay rip-up clasts that can be transported over distances of several kilometers and even tens of kilometers are best when erosion as well as transport occur between approximately 15 to 25 cm/s. Because our experiments were carried out with kaolinite, the results may differ somewhat for other clay mixtures. Also, if strata that are rich in redeposited soft mud clasts extend for more than a few tens of kilometers laterally, one should assume that they must have been replenished by newly eroded material along the transport path.

Owing to the fact that we know that our flume-generated mud fabrics (Figs. 9, 10, 11) originated from piled up water-rich clay rip-up clasts, we can make several generalizations with regard to potential rock-record equivalents. First of all, watery muds that lack appreciable shear strength can still be eroded as fragments and transported by bottom currents. This is an aspect of mudstone sedimentology that has not been considered previously. What is remarkable is that the tested deposits have water contents of approximately 85% by volume, quite similar to the water content of modern ocean muds (e.g., Soutar and Crill 1977; Schimmelmann et al. 1990; Parthenaides 1991). When handled, these muds show no visible resistance and liquefy on touch.

Upon compaction, our mudclast deposits (~ 85% by volume) are likely to show packed upon clasts of lenticular appearance with tapering ends, resulting in a fabric that compares well with lenticular lamination

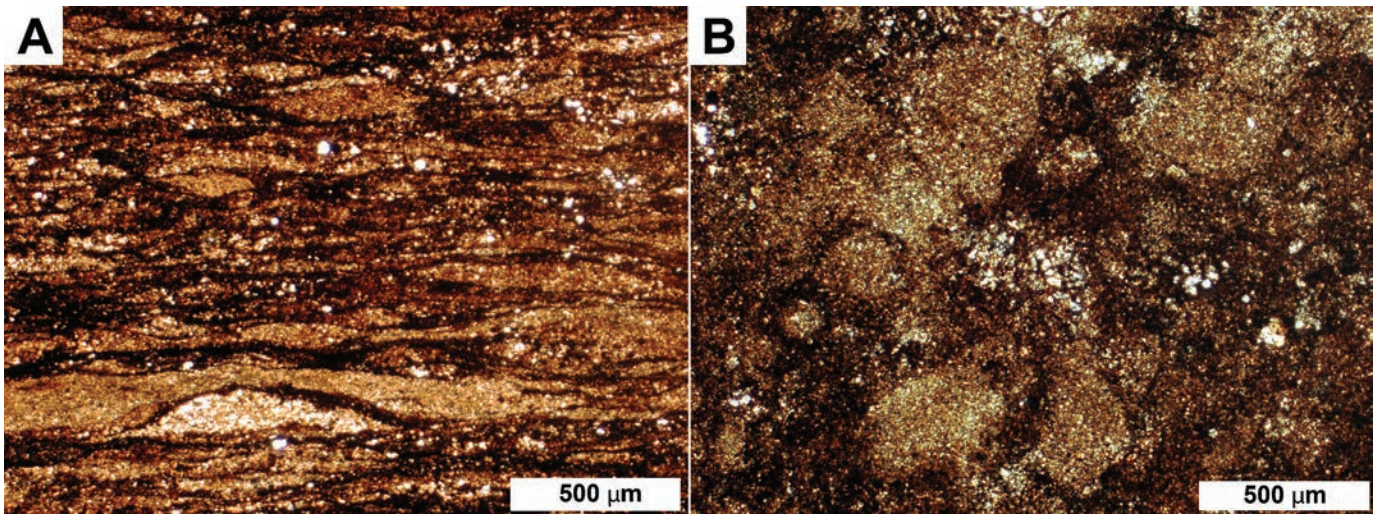

FIG. 12.—Compacted rip-up clasts in the rock record. **A)** Photomicrograph of lenticular laminated Proterozoic shale (Rampur Shale, Vindhyan, India; described by Schieber et al. 2007a) shows well defined compressed clasts that taper and pinch out laterally, very much like the "virtually" compacted experimental deposits in Figures 9 and 10. View is perpendicular to bedding. **B)** Photomicrograph from a thin section cut parallel to bedding (same sample as in Part A. Several shale clasts with irregular outlines are clearly visible (arrows). The sample is poorly sorted.

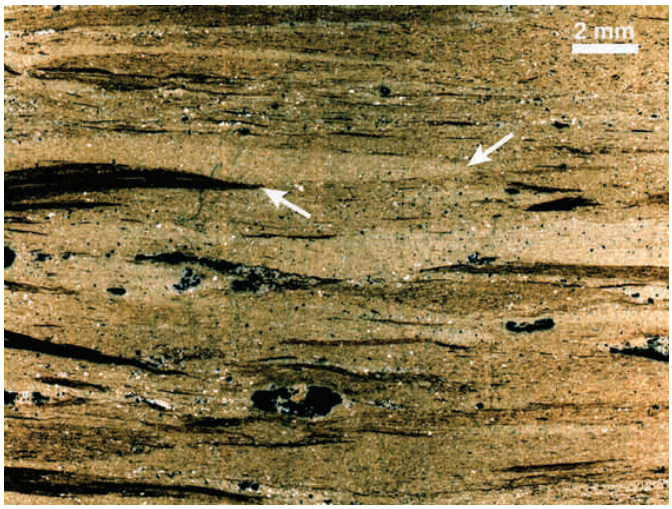

FIG. 13.— A bed of compacted shale clasts from the Eocene Green River Formation of Wyoming. Dark clasts are oil shale fragments. Note vertical compaction, bending of clasts, and tapered edges of clasts (arrows).

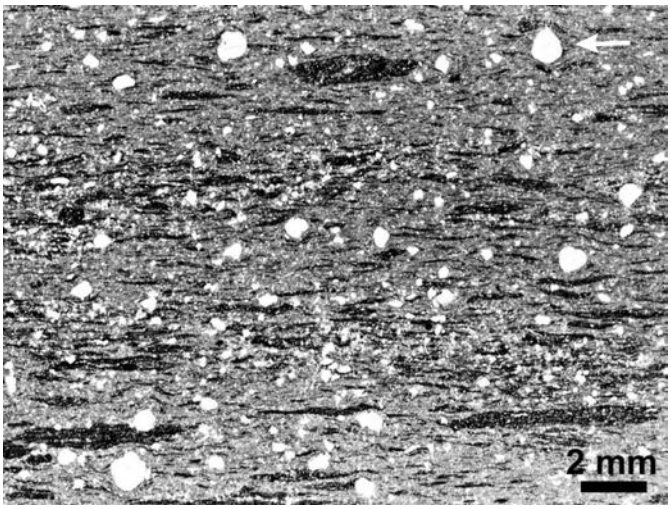

FIG. 14.— Shale with microbial-mat fragments (dark-colored deformed particles; Schieber 1986) and quartz grains (clear) in a matrix of gray shale (Newland Formation, Proterozoic, Montana). Arrow points out differential compaction around quartz grain.

described from the rock record (Fig. 2, and examples in O'Brien and Slatt 1990). Comparing a close-up (Fig. 12) of the same shale pictured in Figure 1 (Proterozoic Rampur Shale, India) to experimental sediments in Figure 9 (approximately the same scale) shows that their fabric closely resembles the lenticular-laminated fabric of its Proterozoic counterpart. In the context of our experiments, extensive formation of lenticular lamination in the Rampur Shale (Sur 2004) implies erosion of water-rich muds over wide areas by bottom currents in the 15 to 25 cm/s range, an interpretation consistent with its offshore marine setting (Sur 2004).

Figure 13 shows an example of lenticular lamination from the Eocene Green River formation of Wyoming, with a mixture of shale clasts that were reworked by waves and currents in a shallow lake-margin setting (Eugster and Hardie 1975). Clasts are strongly flattened, are deformed around other clasts, and show tapered edges. Many of the clasts range in size from 5 millimeters to several centimeters, and the overall fabric compares well to the experimental fabrics seen in Figure 10. The style of clast deformation suggests high water contents of the original clasts. In the context of our experiments, the large clast sizes in this example suggest a short transport distance, consistent with a lake-margin setting.

Because petrographic thin sections permit only a two-dimensional view of rock fabrics, one can of course think of alternative scenarios that would produce the fabrics seen in Figures 2, 12, and 13. For example, various authors have attributed lenticular lamination in the Toarcian Posidonia Shale to deposition of fecal pellets from the water column (e.g., Röhl et al. 2001; Schmid-Röhl 2002). A comparable fabric may also result when a shale with an abundance of subhorizontal burrows undergoes compaction. Fortunately, bedding-parallel thin sections help to sort out these ambiguities. Whereas rip-up clasts would show irregular outlines and poor sorting (Fig. 12B) in plan view, fecal pellets would typically be ovoid in shape, sub-millimeter in size (Cuomo and Bartholomew 1991; Roehl et al. 2001), and of comparatively narrow size distribution. Likewise, the presence of elongate curved features in plan view would suggest compacted burrow tubes rather than clasts or fecal pellets. Thus, whereas lenticular lamination in shales can have multiple origins, petrographic criteria exist that allow us to determine whether in a given case erosion by bottom currents was the underlying cause.

Experimental deposits formed from clasts of plastic mud with significantly lower water content (Fig. 11) are readily distinguished from deposits of water-rich clasts. After "virtual" compaction they still retain their rounded edges, are much less flattened, and are quite similar to ancient deposits of semilithified shale clasts (Fig. 1). They contrast strongly with deposits formed from soft water-rich clasts (Fig. 2). Deposits of eroded and transported consolidated muds are well known from terrestrial settings (e.g., Nanson et al. 1986; Müller et al. 2004; Wright and Marriott 2007) and have also been observed in shallow marine environments (Fig. 1). Such clasts are largely compacted and much more durable than the rip-up clasts described here. As a result they are rounded during transport (like the clasts in Fig. 1) and resist compaction and deformation (e.g., Schieber 1985; Müller et al. 2004).

As long as water-rich mud rip-ups are either large (Fig. 13) or contrasting in color, general flattening (Fig. 2), bending around other clasts (Fig. 12A), tapering lateral terminations (Fig. 12A), and their appearance in plan view (Fig. 12B), should allow their positive identification in the rock record. However, when compositional contrast between fragments is lacking, a shale that originated from current-deposited mud rip-ups may be difficult to recognize. Figure 14 exemplifies this problem. It shows a gray, fine-grained shale matrix, in which we see "suspended" quartz grains and soft, deformed carbonaceous fragments (probably derived from microbial mats; Schieber 1986). If the matrix was just plain flocculated mud deposited simultaneously with large quartz grains, the latter would most likely have settled through the mud until they encountered a horizon sufficiently viscous to stop their descent. Yet, the symmetrical differential compaction observed around these large quartz grains (Fig. 14) shows that this did not happen. The observed texture strongly suggests that the shale matrix surrounding the quartz grains consisted originally of soft mud rip-ups, but that many of these are no longer resolvable at the current state of compaction. The readily recognizable microbial-mat fragments are suggestive of current transport and give an idea of the likely size range of the now "invisible" mud rip-ups. Thus, although lenticular lamination in shales can indicate intermittent erosion and transport of surficial water-rich muds by currents, this important paleoenvironmental clue is easily missed if the eroded shale lacks compositional variability.

CONCLUSION

Whereas one would have assumed that freshly deposited water-rich muds lack the strength to be eroded and transported as larger aggregates, our experiments demonstrate otherwise. Experimental muds with 70 wt.

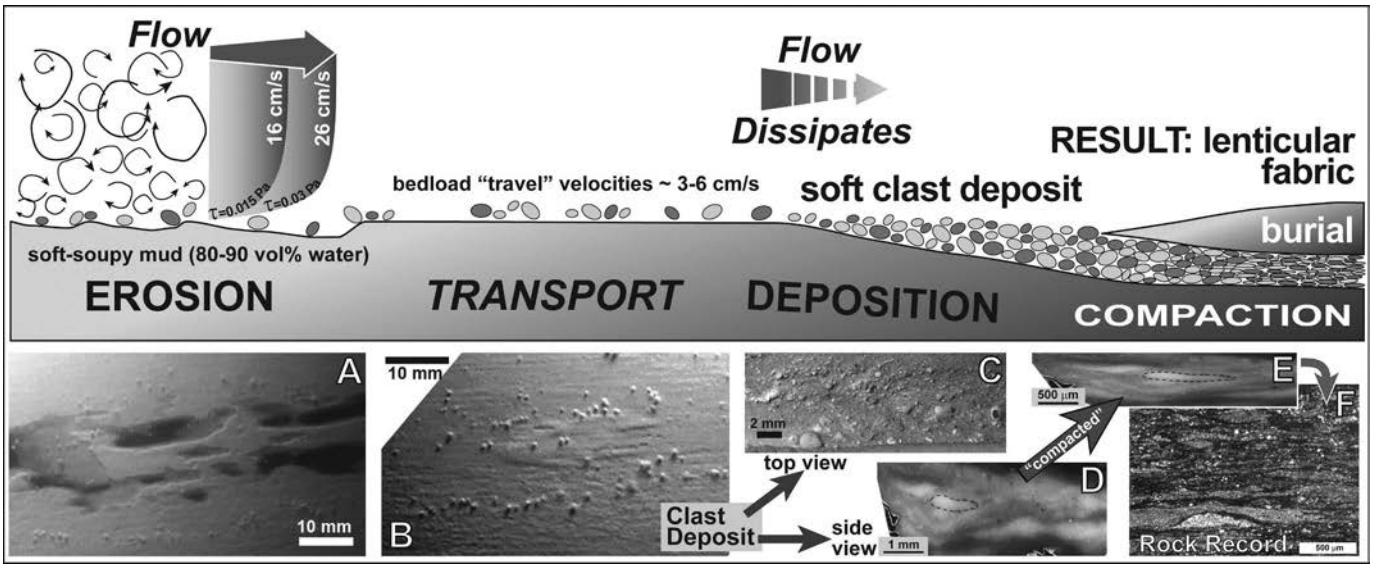

FIG. 15.—A summary of the processes that produce lenticular lamination in shales via erosion and redeposition of water-rich mud clasts. The images along the bottom are examples of depicted processes and outcomes in experiment and rock record.

% water can form millimeter-to centimeter-size fragments upon erosion. Fragment size diminishes during transport, but sand-size to millimeter-size fragments can potentially be transported for tens of kilometers. When these experimental water-rich clay clasts enter an area of lower flow velocity they form deposits of piled-up fragments. Figure 15 summarizes this process and combines it with appropriate imagery from experiments and the rock record. By manipulating digital images of our experimental deposits to simulate compaction, we can show that a lenticular-laminated fabric would result that represents a direct match to lenticular lamination observed in shales from the rock record. Although this fabric may also result from accumulation of fecal pellets and compression of burrow fills, petrographic criteria (using thin sections cut parallel to bedding) allow distinction of those fabrics from lenticular lamination that records intermittent erosion and transport of surficial water-rich muds by currents. Given the widespread occurrence of this fabric in Proterozoic and Phanerozoic shales, application of these criteria to the rock record should allow the identification of many more shale successions that consist of eroded and redeposited mud clasts.

ACKNOWLEDGMENTS

This research was supported by National Science Foundation grants EAR 0308921 and EAR 0617128.

REFERENCES

ALLEN, J.R.L., 1982, Sedimentary Structures: Their Character and Physical Basis: Amsterdam, Elsevier, 2 volumes, 593 p. and 693 p.

BAAS, J.H., AND BEST, J.L., 2002, Turbulence modulation in clay-rich sediment-laden flows and some implications for sediment deposition: Journal of Sedimentary Research, v. 72, p. 336–340.

BERLAMONT, J., OCKENDEN, M., TOORMAN, E., AND WINTERWERP, J., 1993, The characterization of cohesive sediment properties: Coastal Engineering, v. 21, p. 105–128.

BREED, C.S., MCCAULEY, J.F., AND WHITNEY, M.I., 1989, Wind erosion forms, *in* Thomas, D.S.G., ed., Arid Zone Geomorphology: New York, Halstead Press, p. 284–307.

CUOMO, M.C., AND BARTHOLOMEW, P.R., 1991, Pelletal black shale fabrics: their origin and significance, *in* Tyson, R.V., and Pearson, T.H., eds., Modern and Ancient Continental Shelf Anoxia, Geological Society of London, Special Publication 58, p. 221–232.

EINSELE, G., OVERBECK, R., SCHWARZ, H.U., AND UNSÖLD, G., 1974, Mass physical properties, sliding and erodability of experimentally deposited and differently consolidated clayey muds: Sedimentology, v. 21, p. 339–372.

EUGSTER, H.P., AND HARDIE, L.A., 1975, Sedimentation in an ancient playa-lake complex—The Wilkins Peak Member of the Green River Formation of Wyoming: Geological Society of America, Bulletin, v. 68, p. 319–334.

HAWLEY, N., 1981, Flume experiments on the origin of flaser bedding: Sedimentology, v. 28, p. 699–712.

KUEHL, S.A., NITTROUER, C.A., AND DEMASTER, D.J., 1986, Distribution of sedimentary structures in the Amazon subaqueous delta: Continental Shelf Research, v. 6, p. 311–336.

KUEHL, S.A., NITTROUER, C.A., AND DEMASTER, D.J., 1988, Microfabric study of fine-grained sediments: Observations from the Amazon subaqueous delta: Journal of Sedimentary Petrology, v. 58, p. 12–23.

KUEHL, S.A., HARIU, T.M., SANFORD, M.W., NITTROUER, C.A., AND DEMASTER, D.J., 1991, Millimeter scale sedimentary structure of fine-grained sediments: Examples from continental margin environments, *in* Bennett, R.H., Bryant, W.R., and Hulbert, M.H., eds., Microstructure of Fine-Grained Sediments: New York, Springer-Verlag, p. 33–45.

LOBZA, V., AND SCHIEBER, J., 1999, Biogenic sedimentary structures produced by worms in soupy, soft muds: Observations from the Chattanooga Shale (Upper Devonian) and experiments: Journal of Sedimentary Research, v. 69, p. 1041–1049.

MIDDLETON, G.V., AND SOUTHARD, J.B., 1984, Mechanics of sediment movement: SEPM, Short Course 3, 401 p.

MÜLLER, R., NYSTUEN, J.P., AND WRIGHT, V.P., 2004, Pedogenic mud aggregates and paleosol development in ancient dryland river systems: Criteria for interpreting alluvial mudrock origin and floodplain dynamics: Journal of Sedimentary Research, v. 74, p. 537–551.

NANSON, C.G., RUST, B.R., AND TAYLOR, G., 1986, Coexistent mud braids and anastomosing channels in an arid-zone river: Cooper Creek, central Australia: Geology, v. 14, p. 175–178.

O'BRIEN, N.R., AND SLATT, R.M., 1990. Argillaceous Rock Atlas: New York, Springer-Verlag, 141 p.

PARTHENIADES, E., 1991, Effect of bed shear stresses on the deposition and strength of deposited cohesive muds, *in* Bennett, R.H., Bryant, W.R., and Hulbert, M.H., eds., Microstructure of Fine-Grained Sediments: New York, Springer-Verlag, p. 175–183.

PASIERBIEWICZ, K.W., AND KOTLARCZYK, J., 1997, Flume experiments with fine-grained suspension, with applications for the origin of mud laminites: Journal of Sedimentary Research, v. 67, p. 510–513.

RÖHL, H.-J., SCHMID-RÖHL, A., OSCHMANN, W., FRIMMEL, A., AND SCHWARK, L., 2001, The Posidonia Shale (Lower Toarcian) of SW-Germany: an oxygen-depleted ecosystem controlled by sea level and paleoclimate: Palaeogeography, Palaeoclimatology, Palaeoecology, v. 165, p. 27–52.

SCHIEBER, J., 1985, The relationship between basin evolution and genesis of stratiform sulfide horizons in mid-Proterozoic sediments of central Montana (Belt Supergroup) [Ph.D. Dissertation]: University of Oregon, 811 p.

SCHIEBER, J., 1986, The possible role of benthic microbial mats during the formation of carbonaceous shales in shallow Proterozoic basins: Sedimentology, v. 33, p. 521–536.

SCHIEBER, J., 1989, Facies and origin of shales from the Mid-Proterozoic Newland Formation, Belt basin, Montana, U.S.A.: Sedimentology, v. 36, p. 203–219.

SCHIEBER, J., 1998a, Deposition of mudstones and shales: Overview, problems, and challenges, *in* Schieber, J., Zimmerle, W., and Sethi, P., eds., Shales and Mudstones (vol. 1): Basin Studies, Sedimentology and Paleontology: Stuttgart, Schweizerbart'sche Verlagsbuchhandlung, p. 131–146.

Schieber, J., 1998b, Sedimentary features indicating erosion, condensation, and hiatuses in the Chattanooga Shale of Central Tennessee: relevance for sedimentary and stratigraphic evolution, *in* Schieber, J., Zimmerle, W., and Sethi, P., eds., Shales and Mudstones (vol. 1): Basin Studies, Sedimentology and Paleontology: Stuttgart, Schweizerbart'sche Verlagsbuchhandlung, p. 187–215.

Schieber, J., Sur, S., and Banerjee, S., 2007a, Benthic microbial mats in black shale units from the Vindhyan Supergroup, Middle Proterozoic of India: The challenges of recognizing the genuine article, in Schieber, J., Bose, P.K., Eriksson, P.G., Banerjee, S., Sarkar, S., Altermann, W., and Catuneau, O., eds., Atlas of Microbial Mat Features Preserved within the Clastic Rock Record: Amsterdam, Elsevier, p. 189–197.

Schieber, J., Southard, J.B., and Thaisen, K.G., 2007b, Accretion of mudstone beds from migrating floccule ripples: Science, v. 318, p. 1760–1763.

Schimmelmann, A., Lange, C.B., and Berger, W.H., 1990, Climatically controlled marker layers in Santa Barbara Basin sediments and fine-scale core-to-core correlation: Limnology and Oceanography, v. 35, p. 165–173.

Schmid-Röhl, A., Röhl, H.-J., Oschmann, W., Frimmel, A., and Schwark, L., 2002, Paleoenvironmental reconstruction of Lower Toarcian epicontinental black shales (Posidonia Shale, SW Germany): global versus regional control: Geobios, v. 35, p. 13–20.

Segall, M.P., and Kuehl, S.A., 1994, Sedimentary structures on the Bengal shelf: a multi-scale approach to sedimentary fabric interpretation: Sedimentary Geology, v. 93, p. 165–180.

Sheu, D.D., and Presley, B.J., 1986, Variations of calcium carbonate, organic carbon and iron sulfides in anoxic sediment from the Orca Basin, northern Gulf of Mexico: Marine Geology, v. 70, p. 103–118.

Smith, S.J., and Anderson, R.S., 1995, A method for impregnating soft sediment cores for thin section microscopy: Journal of Sedimentary Research, v. 65, p. 576–577.

Soutar, A., and Crill, P.A., 1977, Sedimentation and climatic patterns in the Santa Barbara Basin during the 19th and 20th centuries: Geological Society of America, Bulletin, v. 88, p. 1161–1172.

Spurr, A.R., 1969, A low-viscosity epoxy resin embedding medium for electron microscopy: Journal of Ultrastructure Research, v. 26, p. 31–43.

Sur, S., 2004, An integrated sedimentological, stratigraphical and geochemical study of two Proterozoic black shales from Vindhyan Supergroup [unpublished M.S. thesis]: Bloomington, Indiana, Indiana University, 176 p.

Wignall, P.B., 1989, Sedimentary dynamics of the Kimmeridge Clay: tempests and earthquakes: Geological Society of London, Journal, v. 146, p. 273–284.

Wignall, P.B., 1994, Black shales: Oxford, U.K., Oxford University Press, Geology and Geophysics Monographs, no. 30, 130 p.

Wright, V.P., and Marriott, S.B., 2007, The dangers of taking mud for granted: lessons from Lower Old Red Sandstone dryland river systems of South Wales: Sedimentary Geology, v. 195, p. 91–100.

Received 26 January 2009; accepted 2 September 2009.

ERRATUM: we revisited the shear stress determinations done for this paper, and found that the reported values are most likely too low. Our newer data suggest that for a flow velocity of 16 cm/sec a shear stress of 0.07 Pa is more accurate, and that for 26 cm/sec a value of 0.21 Pa is more appropriate. The basic conclusions are not affected by this change.